Ionic Conductivity of Polymer Complexes Formed by Poly(ethylene succinate) and Lithium Perchlorate

Masayoshi Watanabe,*[1a] Masahiro Rikukawa,[1a] Kohei Sanui,[1a] Naoya Ogata,[1a] Hisaaki Kato,[1b] Tadahiko Kobayashi,[1b] and Zentaro Ohtaki[1b]

Department of Chemistry and Department of Electrical and Electronic Engineering, Sophia University, Tokyo 102, Japan. *Received February 29, 1984*

ABSTRACT: The correlation between molecular characteristics and the electrical conductivity in poly(ethylene succinate)–lithium perchlorate (PE-2,4–$LiClO_4$) complexes was investigated. The PE-2,4–$LiClO_4$ complexes were prepared by dissolvng $LiClO_4$ directly in PE-2,4 above its melting point. The PE-2,4–$LiClO_4$ complexes were semicrystalline polymers with crystallites similar to pure PE-2,4. $LiClO_4$ was dissolved in the amorphous region of PE-2,4. The degree of crystallinity of the PE-2,4–$LiClO_4$ complexes which reached an equilibrium crystallization by annealing decreased in comparison with that of PE-2,4 and was almost independent of the $LiClO_4$ concentration. The dissolution of $LiClO_4$ enhanced T_g and depressed the rate of crystallization of the host polymer. Complex impedance and direct-current measurements with platinum and/or lithium electrodes revealed that the electrical conductivity, which reached the order of 10^{-5} S cm^{-1} at 90 °C, was caused by transport of ionic carriers. The main charge carriers were likely Li^+. Temperature dependences of the conductivity of the PE-2,4–$LiClO_4$ complexes with [$LiClO_4$]/[unit] = 0.02 and 0.04 obeyed the Williams–Landel–Ferry (WLF) equation where C_1 = 11–13 and C_2 = 60–70, which indicated that the temperature dependences were dominated by the ionic mobility correlating with the segmental mobility of the amorphous main chain. The PE-2,4–$LiClO_4$ complexes with higher $LiClO_4$ concentrations showed nearly an Arrhenius behavior in terms of the temperature dependences. The increase in the ion–ion interactions with increasing $LiClO_4$ concentrations induced the conductive behavior which could not be simply interpreted by the WLF equation based on the free volume theory.

Introduction

The continuing development of miniature electronic systems requires parallel improvement in energy sources, sensors, displays, and so on. Solids with high ionic conductivity are called fast-ion conductors or solid electrolytes.[2] They have been attracting much interest because of their potential applications to the above fields and of general interest in mechanisms of the high ionic conductivity. Most fast-ion conductors which have been studied are special inorganic materials such as Ag_4RbI_5 and Na-β-alumina, whose conductivity reached 10^{-2}–10^{-1} S cm^{-1} at relatively low temperatures.[2]

Recently, relatively high ionic conductivity was reported in some polymers.[3-6] The conductivity was lower than that of the special inorganic materials by several orders of magnitude, while a good processability of polymers could enhance the ease and scope of their applications. Most reports of high ionic conductivity in polymers have been concerned with poly(ethylene oxide) (PEO)–alkali metal salt complexes.[5-16] It was found that a stoichiometric ratio of 1 mol of cation to 4 mol of EO repeat unit was required in the ionic polymer complex.[7] The melting point of the complexes ($\simeq$180 °C) was higher than that of pure PEO ($\simeq$ 60 °C).[6,8] The complexation was considered to involve coordination of the cations to the ether oxygen atoms in the polymer backbone, as seen in macrocyclic polyether complexes.[6,9-12] At the initial stage of the study, the high ionic conductivity of the PEO complexes was attributed to the intrahelical jumping process by analogy with fast-ion transport in the inorganic materials.[6] However, evidence that ionic transport within the amorphous region was an important process in the high ionic conductivity was presented by several authors.[13-16] For example, amorphous PEO gels containing the salt showed much higher conductivity than the crystalline complexes,[13,14] and heat treatment that reduced the crystallinity of the complex enhanced the conductivity.[15] Moreover, mixed-anion complexes of PEO containing both ion-pairing and non-ion-pairing anions showed a comparable conductivity to the non-ion-pairing complex.[16]

Table I
Molecular Characteristics of Poly(ethylene succinate)

		GPC data		
polymer	η_{sp}/C^a/(dL g^{-1})	$10^{-4}M_n$	$10^{-4}M_w$	M_w/M_n
PE-2,4	0.29	2.34	6.05	2.59

[a] 0.1 g/10 cm^3 in chloroform at 30 °C.

From the standpoint that ion transport in PEO occurs primarily within the amorphous region, it is expected that polymers which have a large concentration of highly polar groups and low glass transition temperature (T_g) may be other polymeric ionic conductors with a high conductivity at ambient temperatures.[12,17-19] Cooperative interaction of neighboring polar groups and ions may generate many ionic carriers, and the high segmental mobility corresponding to low T_g may enhance a mobility of these carriers. Some polymers such as poly(epichlorohydrin) and poly(ethylene succinate) were proposed as polymeric ionic conductors,[12] but their properties have not been reported in detail as yet.

In this article the relation between molecular characteristics and the electrical conductivity in poly(ethylene succinate)–lithium perchlorate (PE-2,4–$LiClO_4$) complexes is described. The ionic character of the electrical conductivity was demonstrated by using complex impedance and direct-current methods with platinum and/or lithium electrodes. The influence of the molecular characteristics on the temperature dependence of the conductivity was discussed in terms of the free volume theory.

Experimental Section

A. Materials. PE-2,4 was synthesized by polycondensation of dimethyl succinate with ethylene glycol at an elevated temperature. Distilled dimethyl succinate, distilled ethylene glycol (4-fold molar amount of the diester), and 0.15 wt % of calcium acetate and 0.035 wt % of antimony trioxide based on the diester were mixed and heated under nitrogen atmosphere. The temperature of the mixture was kept initially at 180 °C for 3 h to distill methyl alcohol and was then elevated to 230 °C for 1 h to distill excess ethylene glycol. Finally, vacuum (1–2 torr) was applied at 230 °C for 3 h for the polycondensation. The polymer obtained

0024-9297/84/2217-2902$01.50/0

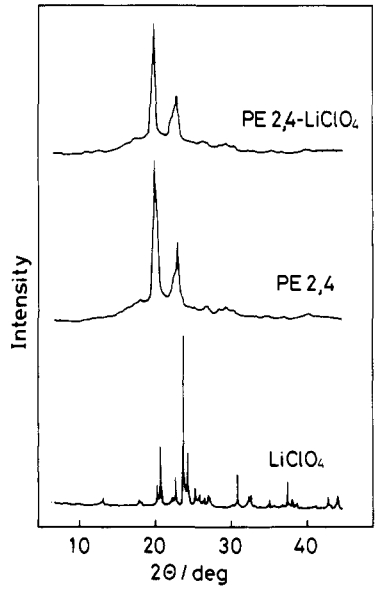

Figure 1. X-ray diffraction patterns of PE-2,4–$LiClO_4$ complex ([$LiClO_4$]/[unit] = 0.08), PE-2,4, and $LiClO_4$.

was purified by reprecipitation using chloroform–methyl alcohol, followed by washing with water and methyl alcohol, repeatedly. This procedure was repeated twice. The sample characteristics are summarized in Table I. The average molecular weights were estimated on a gel permeation chromatograph (Waters Associates, Inc., Model 150C) with a RI detector at 100 °C. The carrier solvent was *m*-cresol. Narrow-distribution polystyrenes were used as the elution standards.

Anhydrous $LiClO_4$ (Mitsuwa Kagaku Co.) was dried under reduced pressure (10^{-3} torr) at 180 °C for 8 h.

B. Preparation of PE-2,4–$LiClO_4$ Complexes. Weighed amounts of PE-2,4 and $LiClO_4$ were mixed and heated under a dry nitrogen stream at 120 °C. $LiClO_4$ gradually dissolved in melt PE-2,4. After the contents became optically homogeneous, it was cooled to room temperature and crushed finely. This procedure was repeated twice in order to achieve homogeneous dissolution of $LiClO_4$ in PE-2,4. The PE-2,4–$LiClO_4$ complexes obtained were annealed under dynamic vacuum at 60 °C for 24 h to reach an equilibrium crystallization. Care was taken to exclude traces of water and standard inert-atmosphere techniques were used during the preparation of the PE-2,4–$LiClO_4$ complexes. The concentration of $LiClO_4$ was expressed as the molar ratio of $LiClO_4$ to repeat unit of PE-2,4 ([$LiClO_4$]/[unit]).

C. Methods. The PE-2,4–$LiClO_4$ complexes were pressed into cylindrical pellets (13 mm in diameter, about 0.3 mm in thickness) for electrical measurements. The pellet sandwiched between platinum and/or lithium electrodes for electrical contacts was packed in a sealed cell with stainless steel terminals which were in contact with the measuring device. The cell assembly was carried out under an inert atmosphere. Alternating-current (ac) measurement was made on the cell with a Hewlett-Packard 4800A vector impedance meter over the frequency range 5 Hz to 500 kHz. Direct-current (dc) measurement was made by applying a constant voltage over the cell and by measuring the current with a Keithley 610C electrometer.

Differential scanning calorimetry was carried out on a DSC apparatus (Rigaku Denki Co., Model 8085) at a heating rate of 20 °C min^{-1}. Powder X-ray diffraction patterns were measured with an X-ray diffractometer (Rigaku Denki Co., Model RAD-IIA). The radiation used was Ni-filtered Cu Kα. Quantitative analysis of lithium was carried out by using an atomic absorption spectrophotometer (Dai-ni Seiko Co., Model SAS-727).

Results and Discussion

A. X-ray Diffraction and Differential Scanning Calorimetry. Figure 1 shows X-ray diffraction patterns of PE-2,4–$LiClO_4$ complex, PE-2,4, and $LiClO_4$. PE-2,4, which had been melted, cooled, and annealed similarly to the PE-2,4–$LiClO_4$ complexes, was a crystalline polymer

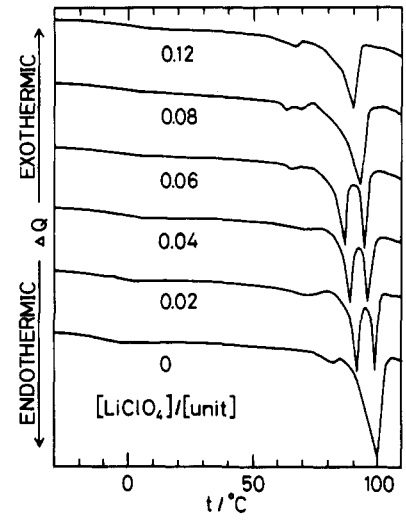

Figure 2. Profiles of differential scanning calorimetry curves of PE-2,4–$LiClO_4$ complexes with various $LiClO_4$ concentrations in the first run. Samples used were previously annealed at 60 °C for 24 h.

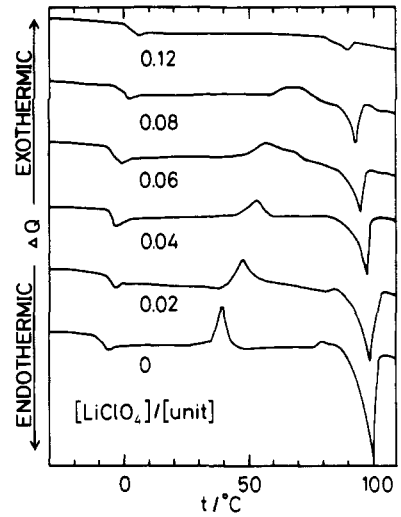

Figure 3. Profiles of differential scanning calorimetry curves of PE-2,4–$LiClO_4$ complexes with various $LiClO_4$ concentrations in the second and third runs. Samples used were quenched from +120 to −100 °C.

and showed sharp diffraction peaks at 2θ = 20.0° and 23.2°. The PE-2,4–$LiClO_4$ complex showed diffraction peaks at the same position as PE-2,4, and no diffraction peaks based on crystalline $LiClO_4$ were observed. The formation of a new crystalline complex as seen in poly(ethylene oxide)–alkali metal salt complexes was not observed. Thus, $LiClO_4$ seemed to dissolve mainly in the amorphous region of PE-2,4.

Results of differential scanning calorimetry (DSC) measurements are summarized in Table II. The profiles of DSC curves of the first run and the second and third runs are shown in Figures 2 and 3, respectively. The samples used in the first run had the same thermal history as those used in the conductivity measurements. The second and third runs were carried out after quenching the samples used in the first and second runs with liquid nitrogen from +120 to −100 °C in the DSC apparatus, respectively. The enthalpy of crystallization and melting were estimated by using phenylazobenzene as a standard substance. This enthalpy for the PE-2,4–$LiClO_4$ complexes was represented as that per unit weight of PE-2,4.

In the first run only melting points (T_m) were clearly determined. The T_m's decreased with the increase in the

Table II
Thermal Properties of PE-2,4 and PE-2,4-$LiClO_4$ Complexes

$[LiClO_4]$/[unit]	run no.	T_g (range)/°C	T_c/°C	ΔH_c[a]/(cal g^{-1})	T_m/°C	ΔH_m[b]/(cal g^{-1})
0	1				100	92.9
	2	−6 (−12 to −3)	39	53.0	101	80.1
			80	12.8		
	3	−7 (−12 to −4)	38	47.6	100	87.1
			79	10.1		
0.02	1				92, 100	68.8
	2	−6 (−10 to −1)	47	54.6	99	76.5
			80	10.2		
	3	−5 (−9 to −1)	47	49.5	100	77.5
			81	10.2		
0.04	1				89, 96	65.3
	2	−3 (−7 to +1)	54	47.8	97	64.7
	3	−2 (−8 to +3)	54	49.2	97	62.9
0.06	1				87, 95	72.1
	2	−1 (−6 to +4)	59	43.7	95	40.7
	3	−1 (−6 to +4)	60	39.4	95	37.2
0.08	1				93	69.2
	2	2 (−4 to +6)	65	21.9	94	21.1
	3	2 (−3 to +5)	65	23.2	93	24.1
0.12	1				90	61.4
	2	5 (−2 to +9)			90	6.1
	3	6 (−1 to +10)			90	4.4

[a] Enthalpy of crystallization. [b] Enthalpy of melting.

$LiClO_4$ concentration. Considering the X-ray diffraction patterns of the PE-2,4–$LiClO_4$ complexes, these T_m's can be assigned to melting of the crystallites of PE-2,4. The decrease in the T_m's may be due to the formation of defects and to the existence of impurity in the crystallites resulting from the dissolution of $LiClO_4$ in PE-2,4. Unfortunately, since the enthalpy of melting (ΔH_m) for the perfectly crystalline PE-2,4 was not available, the degree of crystallinity for the samples could not be quantitatively determined. However, ΔH_m for the PE-2,4–$LiClO_4$ complexes was smaller than that of PE-2,4 and ranged from 61.4 to 72.1 cal g^{-1}. The annealing time did not influence ΔH_m when it was longer than 24 h. This means that the PE-2,4–$LiClO_4$ complexes used reached an equilibrium crystallization with that annealing. Thus, the degree of crystallinity for the PE-2,4–$LiClO_4$ complexes was depressed in comparison with that of PE-2,4 and was almost independent of the $LiClO_4$ concentration. The glass transition temperature (T_g) was not clearly observed in the first run; this may be due to the crystallinity of the samples.

In the second and third runs, T_g, crystallization point (T_c), and T_m were observed in all samples except the PE-2,4–$LiClO_4$ complex of $[LiClO_4]$/[PE-2,4] = 0.12. PE-2,4 had T_g = −7 °C, T_c = 39 and 80 °C, and T_m = 101 °C. The higher T_c might represent metastable crystallization point. ΔH_m was considerably larger than ΔH_c, which suggested that crystallization occurred in the period of quenching. In the PE-2,4–$LiClO_4$ complexes of $[LiClO_4]$/[unit] = 0.02–0.08, T_c increased and ΔH_c decreased with the increase in the $LiClO_4$ concentration. The differences between ΔH_m and ΔH_c became almost negligible in the PE-2,4–$LiClO_4$ complexes of $[LiClO_4]$/[unit] = 0.06 and 0.08. These phenomena showed the rate of crystallization was greatly decreased by the dissolution of $LiClO_4$. Furthermore, T_c was hardly observed in the PE-2,4 complex of $[LiClO_4]$/[unit] = 0.12. T_g's increased from −6 to +6 °C, corresponding to the increase in the $LiClO_4$ concentration. The dissolution of $LiClO_4$ in the amorphous region of PE-2,4 might take place by the ion–dipole interaction. This interaction may suppress the micro-Brownian motion of amorphous main chain.[20-23]

The X-ray and DSC measurements suggested that the PE-2,4–$LiClO_4$ complexes were semicrystalline, but they did not form a new crystalline phase as seen in poly(ethylene oxide)–alkali metal salt complexes.

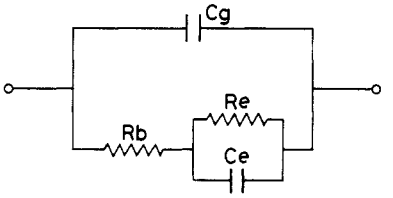

Figure 4. Equivalent circuit to interpret complex impedance diagrams of the samples in the present study: C_g, geometical capacity; R_b, bulk resistance; R_e, electrode/electrolyte interfacial resistance; C_e, electrode/electrolyte interfacial capacity.

B. Ionic Character of Electrical Conductivity. Ions are expected to be main charge carriers in the PE-2,4–$LiClO_4$ complexes. In a solid cell system with ionic carriers, electrode/electrolyte interfacial impedance such as a double-layer capacitance and a charge-transfer resistance must be taken into consideration in addition to bulk electrolyte resistance. Thus, impedance behavior is dependent on frequency and is obtained from ac measurements over a wide range of frequency. The bulk electrolyte impedance is estimated from the corresponding components of an equivalent circuit required to account for the impedance spectrum. We assumed that the equivalent circuit shown in Figure 4 described the impedance behavior of our systems over the frequency range of 5 Hz to 500 kHz. Definitions of C_g, R_b, R_e, and C_e are cited in the figure caption. The impedance (Z) of the equivalent circuit is expressed as

$$Z = \frac{(R_b + R_e) + i\omega R_b R_e C_e}{(1 - \omega^2 R_e C_e R_b C_g) + i\omega(R_b C_g + R_e C_g + R_e C_e)} \quad (1)$$

where ω is the angular frequency, and i is the imaginary unit $(-1)^{1/2}$.

Figure 5 shows the impedance diagrams at 80 °C for the PE-2,4–$LiClO_4$ complex ($[LiClO_4]$/[unit] = 0.08) with a different thickness sandwiched between platinum electrodes. The profile of the diagrams was a semicircle having a low-frequency branch. The resistance values at which reactance took the minimum values changed from 1.36×10^4 to 6.40×10^3 Ω corresponding to the change in the sample thickness from 0.45 to 0.21 mm, and this change

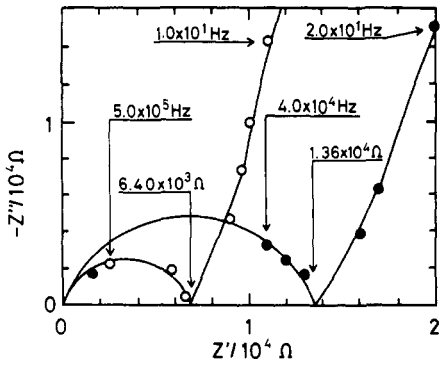

Figure 5. Complex impedance diagrams at 80 °C of PE-2,4-$LiClO_4$ complex ([$LiClO_4$]/[unit] = 0.08) with a different thickness sandwiched between platinum electrodes. Sample thickness: (●) 0.45 mm; (○) 0.21 mm.

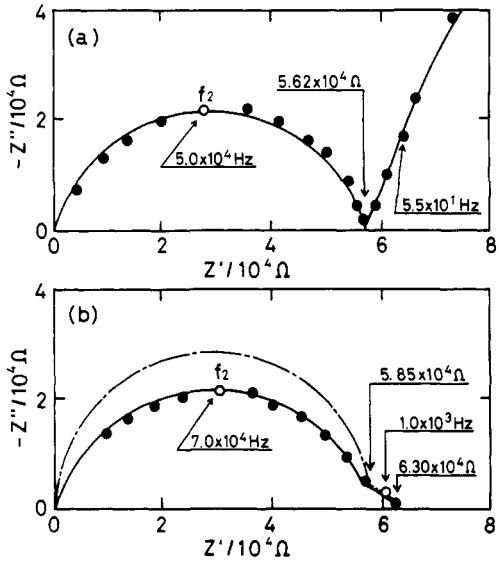

Figure 6. Complex impedance diagrams at 80 °C of PE-2,4-$LiClO_4$ complex ([$LiClO_4$]/[unit] = 0.08) with the same thickness sandwiched between platinum electrodes (a) or lithium electrodes (b). Dashed line in (b) is calculated curve from eq 1 and the values of C_g, R_b, R_e, and C_e.

suggested that the Z' values reflected the bulk resistances of the samples. In Figure 6 are shown the impedance diagrams at 80 °C of the PE-2,4-$LiClO_4$ complex ([$LiClO_4$]/[unit] = 0.08) with the same thickness sandwiched between platinum electrodes (a) or lithium electrodes (b). The high-frequency semicircles were similar in the diagrams of the both cells, whereas the low-frequency impedance was different. In the cell with lithium electrodes (b), one more arc was observed at the low-frequency end of the semicircle. Thus, it was indicated that the low-frequency impedance behavior corresponded to electrode/electrolyte interfacial impedance.

These impedance responses can be interpreted simply on the assumption of $C_g \ll C_e$, which was proposed by Sorensen et al.[24] for the investigation of the impedance behavior of poly(ethylene oxide)–LiSCN complexes. On the basis of this assumption, the equivalent circuit shown in Figure 4 can be reduced to simpler forms, depending on the frequency regions. As shown in Figure 7a, at low frequencies C_g is considered to be open. The equivalent circuit can therefore be symbolized by R_b in series with the parallel combination of R_e and C_e, and eq 1 can be rewritten as

$$Z = R_b + R_e/(1 + i\omega R_e C_e) \quad (2)$$

The profile of the impedance diagram based on eq 2 is the

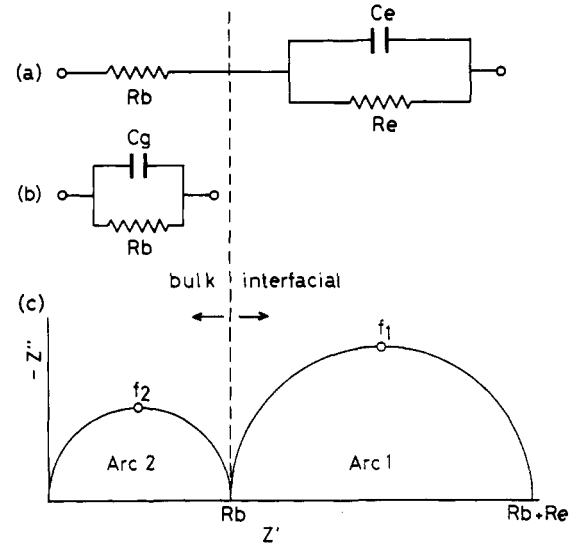

Figure 7. Simplified equivalent circuits at low-frequency region (a) and high-frequency region (b), and corresponding complex impedance diagram (c).

arc 1 centered at $R_g + R_e/2$ on Z' axis with the radius of $R_e/2$, as shown in Figure 7c. The Z' values at low- and high- frequency ends of the semicircle coincide with $R_b + R_e$ and R_b, respectively. f_1 is the relaxation frequency of the parallel combination of R_e and C_e, and is represented by

$$f_1 = 1/2\pi R_e C_e \quad (3)$$

At high frequencies the equivalent circuit is symbolized by the parallel combination of R_b and C_g, and eq 1 is simplified to

$$Z = R_b/(1 + i\omega R_b C_g) \quad (4)$$

The locus of eq 4 is the arc 2 centered at $R_b/2$ on Z' axis with the radius of $R_b/2$. f_2 is related to R_b and C_g as

$$f_2 = 1/2\pi R_b C_g \quad (5)$$

Combining these impedance profiles of both frequency regions, the complete impedance diagram of the equivalent circuit (Figure 4) is obtained as shown in Figure 7c.

On the basis of the above statements, the semicircles of high frequencies in Figures 5 and 6 were found to correspond to the arc 2. The resistance values found from the extrapolation of the semicircles to low frequencies coincided with the bulk electrolyte resistances. The impedance profiles in the low frequencies corresponded to the arc 1. The difference in the profiles depending on the electrodes used (Figure 6) was based on the difference in the values of R_e and C_e. In the case of the cell with platinum electrodes, platinum nearly acted as an ion-blocking electrode. The charge-transfer processes at the electrode/electrolyte interface might proceed with great difficulty, and thus charge-transfer resistance (R_e) was very large. The low-frequency branches seen in Figures 5 and 6a were interpreted as a high-frequency part of the arc 1. On the contrary, in the cell with lithium electrodes, lithium operated as ion-reversible electrodes, and R_e became small. R_b, R_e, f_1, and f_2 in Figure 6b were thus found to be 5.85×10^4 Ω, 4.50×10^3 Ω, 1.0×10^3 Hz, and 7.0×10^4 Hz, respectively. C_g and C_e were estimated from eq 3 and 5 to be 3.89×10^{-11} and 3.54×10^{-8} F. Substituting the values of R_b, R_e, C_g, and C_e to eq 1 allowed the calculated curve (dashed line) in Figure 6b to be obtained. Although we did not take the distribution of the relaxation time into consideration in this calculation, the general profile of the

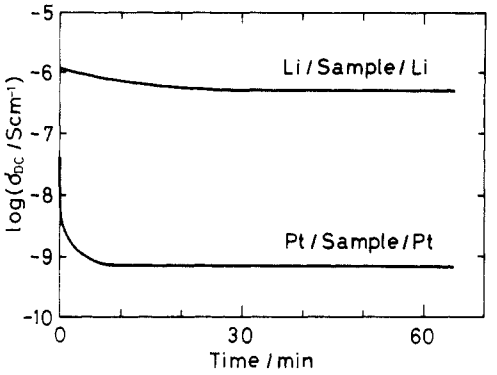

Figure 8. Time dependence of apparent dc conductivity at 80 °C for PE-2,4–$LiClO_4$ complex ([$LiClO_4$]/[unit] = 0.08) with platinum or lithium electrodes.

both diagrams became similar. These results suggested that the impedance behavior could be interpreted by the equivalent circuit shown in Figure 4, and platinum and lithium electrodes operated as ion-blocking and ion-reversible electrodes to the PE-2,4–$LiClO_4$ complexes.

Figure 8 shows the time dependence of apparent dc conductivity at 80 °C estimated from the change in current with time under an applied voltage of 1.0 V. The measurement was carried out on the same samples shown in Figure 6 after the impedance measurement. In the cell with platinum electrodes the conductivity was initially 5.01×10^{-8} S cm^{-1}, followed by the rapid decrease to reach 7.94×10^{-10} S cm^{-1} at about 10 min. Since platinum electrodes block ions and do not block electrons, this decrease might be attributed to a behavior of ionic carriers. The space charge effect of the drifting ions to the electrodes might cause an effective drop of the electric fields in the bulk of the sample, and thus, the conductivity appeared to decrease. Time dependence of dc conductivity of the cell with lithium electrodes was small, compared with that of the cell with platinum electrodes. The constant conductivity reached after about 20 min was 7.08×10^{-7} S cm^{-1}, which was larger than that in the cell with platinum electrodes by 3 orders of magnitude. These results suggested that lithium ion (Li^+) was the charge carrier and that electrode reaction (oxidation and reduction of lithium) and ion migration occurred constantly in the cell with lithium electrodes. Furthermore, the constant conductivity (7.08×10^{-7} S cm^{-1}) obtained in the lithium cell agreed with the conductivity calculated from the resistance (6.30×10^4 Ω) which was assigned to the sum of the bulk resistance (R_b) and the interfacial resistance (R_e) in the complex impedance diagram of the lithium cell, as shown in Figure 6b. Since R_b is determined by the conductance of Li^+ and ClO_4^-, this agreement might show that the conductance of Li^+ mainly contributed to R_b and that Li^+ was main charge carriers.

In order to confirm directly that the PE-2,4–$LiClO_4$ complexes were a Li^+ conductor, the complex was electrolyzed for the cell with a lithium anode and a platinum cathode at an applied voltage of 3.0 V. After an appropriate electrolysis time, the platinum cathode on which lithium was deposited was immersed in a 0.1 N HCl aqueous solution. The amount of the deposited lithium was measured by using the solutions. Figure 9 shows the relation between the amount of deposited lithium onto platinum cathode and the electric charge through the cell. The amount of lithium was in proportion to the electric charge. Thus, it is demonstrated that the PE-2,4–$LiClO_4$ complexes are ionic conductors with Li^+ as the carrier.

C. Temperature Dependence of Electrical Conductivity. Figure 10 shows Arrhenius plot of the electrical

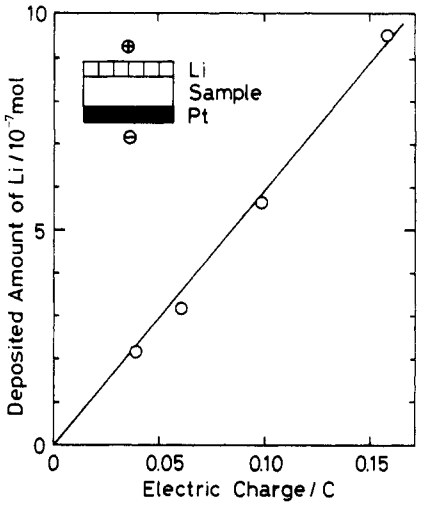

Figure 9. Relation between deposited amount of lithium onto the platinum cathode and electric charge through the cell.

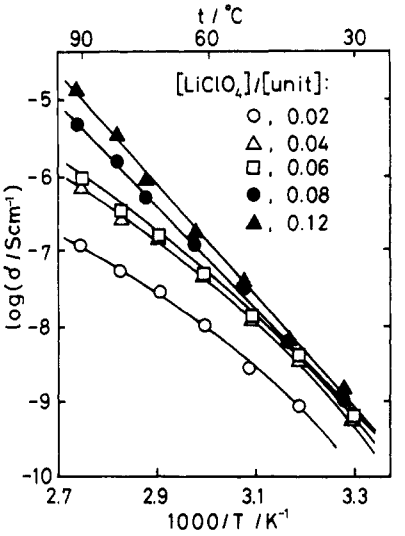

Figure 10. Conductivity of PE-2,4–$LiClO_4$ complexes as a function of reciprocal temperature.

conductivity calculated from the bulk resistance found in the complex impedance measurements. The conductivity increased with the increase in the $LiClO_4$ concentration, and the conductivity of the PE-2,4–$LiClO_4$ complex of [$LiClO_4$]/[unit] = 0.12 reached 10^{-5} S cm^{-1} at 90 °C. The activation energy estimated from the slope of the Arrhenius plot tended to increase with the $LiClO_4$ concentration. However, the temperature dependence could not be explained in terms of classical Arrhenius theory with a temperature-independent activation energy but showed a marked deviation from a single Arrhenius behavior, especially in the samples of low $LiClO_4$ concentrations. It is well-known that temperature dependence of the dielectric or mechanical relaxation time for the micro-Brownian motion of amorphous polymer chains is related to the segmental mobility as represented by the Williams–Landel–Ferry (WLF) equation,[25] based on the free volume theory.[26] $LiClO_4$, which was the origin of charge carriers, was found to dissolve in the amorphous region of PE-2,4, and the measuring temperatures were higher than the T_g's of the corresponding samples. Therefore, the transport of ionic carriers was expected to be related to the segmental mobility of the amorphous chain.

As for temperature dependence of ionic conductivity above T_g, the following equation, in which free volume (V_f), ion–polymer interaction energy (E_i), and ion–ion interac-

Table III
WLF Parameters for PE-2,4-$LiClO_4$ Complexes

$[LiClO_4]$/[unit]	T_g/°C		C_1	C_2/°C	σ_{T_g}/(S cm^{-1})	Δ^a
0.02	onset	−10	12.5	62.4	2.3×10^{-15}	3.2×10^{-2}
	center	−6	11.8	66.5	1.3×10^{-14}	3.2×10^{-2}
	end	−1	10.9	71.9	9.0×10^{-14}	3.2×10^{-2}
0.04	onset	−7	12.9	63.5	1.0×10^{-14}	2.4×10^{-2}
	center	−3	12.1	67.3	6.0×10^{-14}	2.4×10^{-2}
	end	1	11.5	71.3	2.9×10^{-13}	2.4×10^{-2}
0.06	onset	−6	13.9	105	2.6×10^{-13}	2.8×10^{-2}
	center	−1	12.6	86.0	3.0×10^{-13}	3.2×10^{-2}
	end	4	11.8	90.2	1.4×10^{-12}	3.3×10^{-2}
0.08	onset	−4	21.7	209	7.4×10^{-13}	2.0×10^{-2}
	center	2	21.0	215	2.9×10^{-12}	2.0×10^{-2}
	end	6	20.7	217	7.1×10^{-12}	2.1×10^{-2}
0.12	onset	−2	114	1590	7.0×10^{-12}	2.2×10^{-2}
	center	5	125	1770	2.3×10^{-11}	2.2×10^{-2}
	end	9	119	1680	4.3×10^{-11}	2.2×10^{-2}

[a] Deviation (Δ) is defined as $\Delta = [\sum(\log \sigma_{calcd} - \log \sigma)^2/n]^{1/2}$ where σ_{calcd} is the calculated conductivity from eq 9 and the parameters obtained (C_1, C_2, and σ_{T_g}), and n is the number of data points.

tion energy (W) were taken into consideration, had been presented by Miyamoto et al.[27]

$$\sigma(T) = \sigma_0 \exp\left[-\left(\frac{\gamma V_i^*}{V_f} + \frac{E_j + W/2\epsilon}{kT}\right)\right] \quad (6)$$

where σ_0 is a constant, γ is the numerical factor, V_i^* is the critical volume required for transport of an ion, ϵ is the dielectric constant, and k is Boltzmann's constant. V_f is represented by

$$V_f = V_g[f_g + \alpha(T - T_g)] \quad (7)$$

where V_g is the specific volume at T_g, f_g is the free volume fraction at T_g, and α is the expansion coefficient of free volume. If the contribution of the terms of E_j and W to the temperature dependence of the conductivity is assumed to be negligible compared with that of the terms of V_f, the ratio of $\sigma(T)$ to $\sigma(T_g)$ is derived from eq 6:

$$\log \frac{\sigma(T)}{\sigma(T_g)} = \frac{1}{2.303}\left(\frac{\gamma V_i^*}{V_{f_g}} - \frac{\gamma V_i^*}{V_f}\right) \quad (8)$$

where V_{f_g} is the free volume at T_g. Substituting eq 7 to eq 8, we can obtain the following eq 9:

$$\log \frac{\sigma(T)}{\sigma(T_g)} = \frac{(\gamma V_i^*/2.303 V_g f_g)(T - T_g)}{f_g/\alpha + (T - T_g)} = \frac{C_1(T - T_g)}{C_2 + (T - T_g)} \quad (9)$$

which is considered to be the WLF equation for conductivity. Equation 9 was adopted to interpret the temperature dependence of the conductivity of PE-2,4-$LiClO_4$ complexes. Since $\sigma(T_g)$ of the present samples was too low to be measured from the complex impedance method, the data sets of C_1, C_2, and $\sigma(T_g)$ were so calculated as to linearize the correlation between $1/(T - T_g)$ and $1/\log [\sigma(T)/\sigma(T_g)]$. Table III shows the WLF parameters obtained. Glass transition of the PE-2,4-$LiClO_4$ complexes had some temperature width, and thus these calculations were carried out by using the temperatures of onset, center, and end of T_g on each sample. The temperature dependence of the conductivity was represented very well by the WLF equation with small deviation. The WLF parameters of C_1 and C_2 in PE-2,4-$LiClO_4$ complexes with $[LiClO_4]$/[unit] = 0.02 and 0.04 were comparable to the universal values for the temperature dependence of the segmental mobility, that is, $C_1 = 17.4$ and $C_2 = 51.6$.[25] This implies that the temperature dependence was dominated by the ionic mobility which correlated to the segmental mobility of the amorphous main chain. For the complexes with $[LiClO_4]$/[unit] = 0.08 and 0.12, the deviation of the WLF parameters from the universal values is apparent. The temperature dependence approached Arrhenius behavior, as can be seen from Figure 10. The terms of W might become larger in eq 6 and could not be negligible, since the distance between carrier became small with the increase in the $LiClO_4$ concentration. Thus, the conductive behavior could not be simply interpreted by the WLF equation based on the free volume theory.

It can be concluded that the relatively high conductivity comparable to PEO–alkali metal salt complexes was obtained in the PE-2,4-$LiClO_4$ complexes. The conductivity was dominated by ion transport in the amorphous region of PE-2,4 with a high concentration of polar groups with low T_g.

References and Notes

(1) (a) Department of Chemistry. (b) Department of Electrical and Electronic Engineering.
(2) For example: Farrington, G. C. *Science (Washington, D.C.)* **1979**, *204*, 1371. Vashishta, P., Mundy, J. N., Shenoy, G. K., Eds. "Fast Ion Transport in Solids"; North-Holland Publishing Co.: Amsterdam, 1979. Subbarao E. C., Ed. "Solid Electrolytes and Their Applications"; Plenum Publishing Co.: New York, 1980. Haggenmuller, P., Gool, W. V., Eds. "Solid Electrolytes"; Academic Press: New York, 1978.
(3) Watanabe, M.; Kanba, M.; Nagaoka, K.; Shinohara, I. *J. Appl. Polym. Sci.* **1982**, *27*, 4191.
(4) Watanabe, M.; Kanba, M.; Nagaoka, K.; Shinohara, I. *J. Polym. Sci., Polym. Phys. Ed.* **1983**, *21*, 939.
(5) Wright, P. V. *Br. Polym. J.* **1975**, *7*, 319.
(6) Armand, M. B.; Chabagno, J. M.; Duclot, M. J. In "Fast Ion Transport in Solids"; Vashishta, P., Mundy, J. N., Shenoy, G. K., Eds.; North-Holland Publishing Co.: Amsterdam, 1979; pp 131–136.
(7) Fenton, D. E.; Parker, J. M.; Wright, P. V. *Polymer* **1973**, *14*, 589.
(8) Chiang, C. K.; Davis, G. T.; Harding, C. A.; Aarons, J. Fourth International Conference on Solid State Ionics, Grenoble, France, July 4–8, 1983.
(9) Papke, B. L.; Ratner, M. A.; Shriver, D. F. *J. Phys. Chem. Solids* **1981**, *42*, 493.
(10) Papke, B. L.; Ratner, M. A.; Shriver, D. F. *J. Electrochem. Soc.* **1982**, *129*, 1694.
(11) Parker, J. M.; Wright, P. V.; Lee, C. C. *Polymer* **1981**, *22*, 1305.
(12) Shriver, D. F.; Papke, B. L.; Ratner, M. A.; Dupon, R.; Wong, T.; Brodwin, M. *Solid State Ionics* **1981**, *5*, 83.
(13) Lee, C. C.; Wright, P. V. *Polymer* **1982**, *23*, 681.
(14) Payne, D. R.; Wright, P. V. *Polymer* **1982**, *23*, 690.
(15) Weston, J. E.; Steele, B. C. H. *Solid State Ionics* **1982**, *7*, 75.
(16) Dupon, R.; Papke, B. L.; Ratner, M. A.; Whitmore, D. H.; Shriver, D. F. *J. Am. Chem. Soc.* **1982**, *104*, 6247.
(17) Watanabe, M.; Ikeda, J. *Polym. J.* **1983**, *15*, 65.
(18) Watanabe, M.; Ikeda, J. *Polym. J.* **1983**, *15*, 175.

(19) Watanabe, M.; Nagaoka, K.; Kanba, M.; Shinohara, I. *Polym. J.* **1982**, *27*, 4191.
(20) Eisenberg, A.; King, M. "Ion-Containing Polymers"; Academic Press: New York, 1977.
(21) Moacanin, J.; Cuddihy, E. F. *J. Polym. Sci., Part C* **1966**, *14*, 313.
(22) Hannon, M. J.; Wissbrum, K. F. *J. Polym. Sci., Polym. Phys. Ed.* **1975**, *13*, 113.
(23) Wetton, R. E.; James, D. B.; Whiting, W. *J. Polym. Sci., Polym. Lett. Ed.* **1976**, *14*, 557.
(24) Sorensen, P. R.; Jacobsen, T. *Electrochim. Acta* **1982**, *27*, 1671.
(25) Williams, M. L.; Landel, R. F.; Ferry, J. D. *J. Am. Chem. Soc.* **1955**, *77*, 3701.
(26) Cohen, M. H.; Turnbull, D. *J. Chem. Phys.* **1959**, *31*, 1164.
(27) Miyamoto, T.; Shibayama, K. *J. Appl. Phys.* **1973**, *44*, 5372.

Ionic Conductivity of Polymer Complexes Formed by Poly(β-propiolactone) and Lithium Perchlorate

Masayoshi Watanabe,*[1a] Makiko Togo,[1a] Kohei Sanui,[1a] Naoya Ogata,[1a] Tadahiko Kobayashi,[1b] and Zentaro Ohtaki[1b]

Department of Chemistry and Department of Electrical and Electronic Engineering, Sophia University, Kioi-cho, Chiyoda-ku, Tokyo 102, Japan. *Received April 17, 1984*

ABSTRACT: The correlation between molecular characteristics and electrical conductivity in poly(β-propiolactone)–lithium perchlorate (PPL–$LiClO_4$) complexes was investigated. The complex impedance and direct current measurements on a cell made of the PPL–$LiClO_4$ complex sandwiched between platinum and/or lithium electrodes revealed that the electrical conductivity was due to migration of Li^+ with a transference number of nearly unity. It was found that the dissolution of $LiClO_4$ in PPL facilitated the formation of a new crystalline phase with a higher enthalpy of melting than that of pure PPL. The degree of crystallinity decreased with increasing $LiClO_4$ concentration. The temperature dependence of the conductivity showed Arrhenius-type behavior in the low-concentration complex, while it showed WLF-type behavior in the high-concentration complex. The enhancement of conductivity by quenching implied that ion migration in the amorphous region was the main contribution to the ionic conductivity. A maximum conductivity of 3.7×10^{-4} S cm^{-1} was observed in the quenched complex at 70 °C.

Introduction

It is well-known that electrical conduction in ordinary polymers at low electric fields is due to migration of ions originating from ionic impurities in the bulk, absorbed moisture, and decomposition products of polymers.[2-6] The conduction current in these polymers is extremely low, and thus, polymeric materials have been used in electrical fields as insulators or dielectrics. However, a relatively high ionic conductivity was recently reported in ion-containing polymers such as poly(ethylene oxide)- and poly(propylene oxide)–alkali metal salt complexes.[7-10] These findings have stimulated increasing interest in ion-containing polymers with high ionic conductivity because of their potential applications to primary or secondary solid-state batteries, electrochemical displays, and so on.

It was demonstrated by several authors[11-14] that the high ionic conductivity of the polyether complexes could be attributed to ion transport within amorphous regions of the polymers. The segmental mobility of the polyethers with low glass transition temperatures ($T_g \simeq -60$ to -70 °C) is very high at ambient temperatures, which contributes to high mobility of ionic carriers. Structural characteristics such as the polar ether oxygen which exists at every three atoms in the polymer backbone, ensure a cooperative interaction of neighboring oxygen atoms to ions by analogy with the macrocyclic polyethers. This interaction seems to contribute to the generation of a large number of ionic carriers. Thus, the polymers which have both a high concentration of highly polar groups and a low T_g are expected to be ionic conductors in the polymer–salt systems.

In an earlier article,[15] we reported that poly(ethylene succinate)–lithium perchlorate (PE-2,4–$LiClO_4$) complexes had a relatively high ionic conductivity comparable to that of poly(ethylene oxide)–lithium salt complexes. $LiClO_4$ was dissolved in the amorphous region of PE-2,4 but did not form a new crystalline phase with the polymer. The conductivity was attributed to an ion transport process in the amorphous region. As a result, the temperature dependence of the conductivity obeyed a Williams–Landel–Ferry(WLF)-type equation. In this study, poly(β-propiolactone) (PPL) which had a similar structure to PE-2,4 was selected as the host polymer to $LiClO_4$. Lithium ion (Li^+) conduction in the PPL–$LiClO_4$ complexes was demonstrated by means of complex impedance and direct current (dc) measurements on a cell with platinum and/or lithium electrodes. The correlation between molecular characteristics and the temperature dependence of the conductivity was investigated.

Table I
Characterization of Poly(β-propiolactone)

abbrev	η_{sp}/C^a (100 cm^3 g^{-1})	GPC data $M_n/10^4$	$M_w/10^4$	M_w/M_n
PPL	0.43	1.90	4.76	2.50

[a] 0.1 g/10 cm^3 in chloroform at 30 °C.

Experimental Section

A. Materials. PPL was synthesized by means of ring-opening polymerization at a low temperature with diethylzinc/water as a catalyst.[16]

A *n*-hexane solution containing 0.5 mol % diethylzinc was prepared under a dry nitrogen atmosphere. A 57-cm^3 portion of the solution was transferred by a trap-to-trap method into a polymerization tube with a side tube sealed with a rubber cap and was cooled to 0 °C. An equimolar amount of water was added through the side tube by using a microsyringe. The content was sonicated to yield a pale yellow precipitate and was cooled to −30 °C. A 21-g (0.3 mol) quantity of freshly distilled β-propiolactone was

0024-9297/84/2217-2908$01.50/0